



ORIGINAL RESEARCH ARTICLE

# Improving Surface Quality and Fatigue Life of Electron Beam Melted Ti6Al4V by Chemical Machining

Emanuele Manco, Fabio Scherillo , Stefania Franchitti, and Rosario Borrelli

Submitted: 26 May 2023 / Revised: 2 October 2023 / Accepted: 6 October 2023

**Due to the high demand for innovative parts from the aerospace, biomedical, and automotive industries, 3D printing of titanium parts is widely researched. Electron beam melting (EBM) is one of the few additive manufacturing techniques that can quickly generate high density components. However, additive manufacturing techniques based on powder beds are characterized by subpar surface finishing, which also results in poor mechanical performances that are not suitable for industrial standards. Thus, surface finishing post processing is generally needed. Since fatigue behavior is strongly affected by surface quality, this work aims to highlight how chemical machining impacts this type of mechanical response. Rotating fatigue beam testing method has been chosen for the experimental campaign since it intrinsically stresses more the sample surfaces, in this way the effect of surface finishing is highlighted.**

**Keywords** chemical machining, electron beam melting, rotating beam fatigue testing, surface finishing, Ti6Al4V

## 1. Introduction

Metal additive manufacturing (AM) methods offer a fundamental shift in established manufacturing paradigms, especially for structural elements. The advantages of using AM techniques are primarily in the efficient use of materials, high design flexibility, and property customization. Compared to the various raw materials used in conventional manufacturing processes, these advantages are even more evident if powders are used as feedstock because they are flexible, can be manipulated locally, and produce relatively little material waste.

Despite its advantages, structural component design is still in its infancy, especially for periodically loaded parts. In recent years, the interest of companies in the use of additive manufacturing (AM) for both prototyping and mass production has increased the volume of components manufactured in this way and their quality (Ref (1-4)). When compared to the fatigue behavior of traditional materials, AM parts behavior is poor and requires further exploration (Ref (5, 6)). This is because a variety of flaws, particularly surface roughness, porosity, unmelted powders, and others, can affect the fatigue limit.

Titanium, which has outstanding mechanical qualities, corrosion resistance, and biocompatibility, is one of the most

utilized metals in AM (Ref (6-8)). The automotive, aerospace, and biomedical industries are typical fields of application.

Electron Beam Melting (EBM) is a rising AM technology since the vacuum chamber facilitates the manufacturing of parts with high density; however, surface roughness is typically worse when compared to other powder bed fusion technologies. The possibility to 3D print titanium alloys creates new opportunities for designing and manufacturing of load carrying components (Ref (9)), but fatigue behavior needs to be further investigated (Ref (10, 11)). Most studies (Ref (12, 13)) are based on the investigation of the build direction influence on fatigue performance, some researchers focus attention on the influence of beneficial heat treatments to reduce the dimensions of internal defects (Ref (14, 15)). Regarding surface modification treatments (Ref (9)), researchers in literature have extensively investigated the impact of machining while there's a considerable gap of knowledge the fatigue behavior of additively manufactured parts after tool-less treatments, especially chemical finishing.

A lot of methods are studied in the literature to limit the existence of internal defects, control microstructure, and/or reduce surface roughness, which are specifically intrinsic characteristics of all 3D printing techniques. Thermal treatments can be used to control the quality of bulk materials; hot isostatic pressing is one of the most used, it reduces the size of internal pores (Ref (16, 17)) and encourages recrystallization, however, thermal treatments by themselves generally are not sufficient to increase fatigue performances because superficial imperfections are not affected by the treatment.

According to current state of the art, there are several methods for surface post processing of metal AM components, regardless of the method, they can be classified according to their type of interaction with the parts, such as mechanical, thermal, chemical/electrochemical, or a mixture of these.

Mechanical contact treatments are the most used methods, but they are not suitable for complex geometries typical of AM parts. CNC machining (Ref (18)), shot peening (Ref (19, 20)), vibratory polishing, and sandblasting (Ref (21)) are the most common processes in this category. Given the challenging and

**Emanuele Manco** and **Fabio Scherillo**, Department of Chemical, Materials and Industrial Production Engineering, University of Naples "Federico II", P.le Tecchio 80, 80125 Naples, Italy; and **Stefania Franchitti** and **Rosario Borrelli**, Manufacturing Processes of Metallic Materials Lab, Department of Structures and Materials, CIRA, Via Maiorise, 81043 Capua, CE, Italy. Contact e-mail: fabio.scherillo@unina.it.

complex properties of AM metal components, various methods used in other fields are an attractive topic for surface treatment. Fluidized bed, hydrodynamic cavitation grinding and abrasive flow machining techniques are examples (Ref (22-25)). Except for the latter techniques, mechanically based surface treatments have significant limitations in terms of physical access of tools and abrasives to complex shaped components that can be achieved by AM. The same can be said for surface treatments based on thermal interaction. This area is primarily concerned with laser polishing, a process based on surface remelting.

Laser polishing provides better process control than other methods because the characteristics of the laser source are accurate and process parameters, for example laser power, scan speed, overlap between tracks, etc., can be easily regulated. This feature is highly desirable for a smoothing technique applied to a surface with random texture, such as that produced by AM processes; however, as with various mechanical treatments, the application of laser polishing is hindered by the need for physical access of the laser beam to intricate internal structures, and for this reason, the number of possible applications is limited. Given on these assumptions, numerous authors (Ref (26-28)) have studied laser polishing performance for different materials.

Chemical surface treatments, on the other hand, remain one of the most promising methods for homogeneous smoothing of complex parts and surfaces, such as lattice structures. The fundamental perk of chemical treatments relies on the mobility of ions in aggressive solutions, which can be precisely regulated and enhanced when controlled by an electric potential (Ref (29)). Scherillo et al studied the chemical polishing on AlSi10Mg specimens fabricated by SLM and Ti6Al4V fabricated by EBM with a simple geometry and found a significant improvement in surface quality as measured by various indicators (Ref (30, 31)). In addition, Wysocki et al (Ref (32)) demonstrated the efficacy of chemical processing in improving the surface quality of Ti6Al4V scaffolds fabricated by EBM and the ability of the treatment to integrate bone cells.

In conclusion, post processing procedures are widely investigated in literature, and they are often effective. Examples of this may be seen in Obeidi et al research on laser polishing, which shows that the surface roughness of Ti6Al4V specimens generated by laser powder bed fusion can be decreased from the initial value by up to 90% (Ref (33)) (final Sa of 3  $\mu\text{m}$  for both flat and cylindrical specimens). Most analyses of fatigue life have compared as-built specimens to machined ones, and, as demonstrated by several authors (Ref (16, 34, 35)), machined specimens often exhibit improved fatigue behavior; however, tool-less treatments should be preferred to most of the conventional processes since they are not suited for complex shapes, such as ones that may be advantageously achieved by additive manufacturing.

The contribution of this work is intended to fill gap of knowledge regarding the influence of chemical machining treatments and particularly  $\text{HNO}_3$ /HF based solutions for EBM Ti6Al4V since few works currently investigated the influence

of treatment on fatigue life for SLM parts (Ref (36, 37)) while researches such as Rony et al.'s are focused on surface cleaning/polishing by removing unmelted particles by means of acid treatment (Ref (38)).

In this research, the influence of chemical surface finishing for Ti6Al4V has been investigated and related to fatigue performances after treatment. In order to highlight the surface quality contribution for fatigue behavior, rotating beam fatigue tests have been carried out on chemically treated EBM Ti6Al4V specimens and their behavior has been compared to as-built EBM Ti6Al4V tested in the same way.

Fatigue behavior of treated parts resulted enhanced if compared to untreated parts, in addition, the chemical process is capable of reaching similar results to conventional machining or other mechanical treatments on Ti6Al4V EBM parts (Ref (37)).

## 2. Materials and Methods

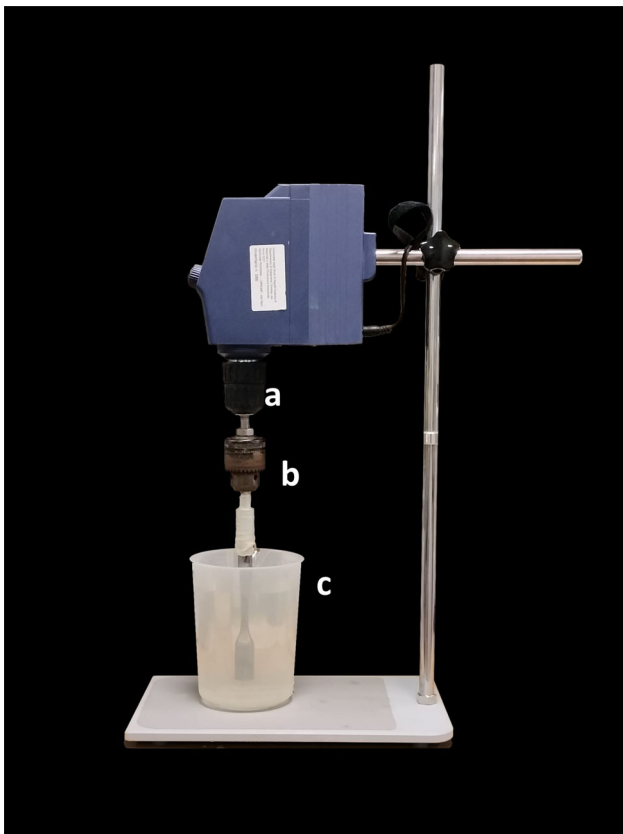
EBM was used to print the samples tested for this work, feedstock material was Ti6Al4V powders (powder size ranging from 45 to 106  $\mu\text{m}$ ), whose composition is listed in Table 1. For this project, the Italian Aerospace Research Center (CIRA) provided an ARCAM A2X EBM machine. The samples manufacturing was carried out in a vacuum chamber with a pressure of  $10^{-4}$  mbar and were made using standard Ti6Al4V melting themes. Beam current and beam velocity were adjusted to keep the energy density constant at a value of 40  $\text{J}/\text{mm}^3$  according to algorithms developed by the manufacturer in an effort to achieve full dense as-built parts with consistent microstructure and properties.

Since the algorithm is covered by copyright, beam current and beam speed time-dependent diagrams are hidden to the users. The beam employs a back-and-forth raster pattern. The raster pattern changes direction every layer: the beam moves parallel to the x-direction for the first layer and it moves along y-direction for the subsequent layer. A line offset of 0.1 mm was set. Wafer mounts were used to aid in heat dissipation. Finally, the samples were scaled to account for thermal shrinkage (ARCAM recommended scaling factors: 1.0092 for the x and y directions and 1.0132 for the z direction), the layer thickness was of 50  $\mu\text{m}$ . During the EBM process the entire build is kept at elevated temperatures, assuring a correct microstructure and parts free from residual stresses, hence no post process heat treatment was performed after manufacturing. Materialize Magics software was used to set the orientation and position of the parts in the build chamber.

To lessen the impact of the staircase effect and ensure the best vertical alignment of the samples (Ref (39)), they were created vertically in the build chamber and their geometry was designed according to ISO1143 rotating bending fatigue standard. No contour plan optimization was used to deal with the worst surface quality possible.

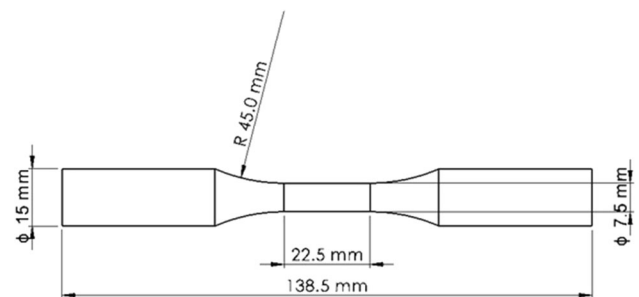
**Table 1** Composition of Ti6Al4V powders

Element	Al	V	Fe	O	N	H	C	Ti
Wt%	6.40	4.12	0.18	0.14	0.01	0.003	0.01	Balance

**Fig. 1** Detailed setup of chemical machining procedure: (a) rotating spindle, (b) sample holder with fatigue specimen, (c) acidic solution

Samples were cut by means a metallographic abrasive cutter and the parallel and orthogonal sections, to respect additive growing direction, were observed using Hitachi TM 3000 electron microscope and Zeiss Axioplan optical microscope. Before observation the sample were polished to mirror like finishing and etched using a solution made of H<sub>2</sub>O and 1 ml HF (48 wt%). On as polished samples micro-hardness measurements were conducted using a CV Instrument micro-hardness tester and an indentation force of 500 g.

The effect of fluid velocity on the capability of chemical machining to reduce surface roughness of EBM samples was studied in detail, to this aim cylindrical shaped samples with initial diameter of 8 mm were immersed in the acidic solution and put in rotation around their ax for 90 min according to setup reported in Fig. 1.

**Fig. 2** Detailed geometry of fatigue specimen

Three different conditions were analyzed: high rotational speed (HRS) corresponding to 450 RPM, low rotational speed (LRS) corresponding to 50 RPM and finally stagnant (ST). An HF-HNO<sub>3</sub> aqueous solution (HF (48 wt%) 28 ml, HNO<sub>3</sub> (69 wt%) 225 ml, H<sub>2</sub>O 736 ml) was employed.

Every 15 minutes, the diameter reduction was measured, and surface topology was acquired in a covered area of 3X10 mm<sup>2</sup>. The effect of the treatment was studied by observing the total Sa, roughness (Ra), and waviness (Wa) surfaces, by the use of Leica DCM 3D confocal microscope and LeicaMap software. Wa and Sa were separated applying Gaussian filter with a cut-off of 0.08 mm.

The as-built AM Ti6Al4V fatigue behavior is well studied in the literature, and it is well known that surface finishing of parts has an impact on fatigue life, particularly the life under high cycle fatigue (HCF) conditions (Ref (40)). The tests have been performed using an experimental rotating beam fatigue testing setup, designed, and produced in collaboration with a local company. Constant amplitude rotating beam fatigue testing was performed with a stress ratio of  $R = -1$  while load frequency was set to 70 Hz at room temperature, similarly to a previous work from the authors regarding axial fatigue testing (Ref (41)). Three different stress levels have been investigated: the maximum stress tested was 900 MPa to determine the LCF fatigue limit (around the 10<sup>3</sup> cycles life); 300 MPa was set to highlight the fatigue limit (considering 10<sup>7</sup> cycles as runout) according to preliminary results from the above mentioned work and literature findings (Ref (6, 42, 43) for AM Ti6Al4V fatigue tests, and a middle stress level was imposed at 500 MPa to provide further information to the experimental curve. The as-built and treated specimens fatigue curves were obtained by testing three specimens for each stress level, finally HITACHI TM3000 scanning electron microscope and Nikon SMZ 745T stereomicroscope were used to examine the fracture surfaces

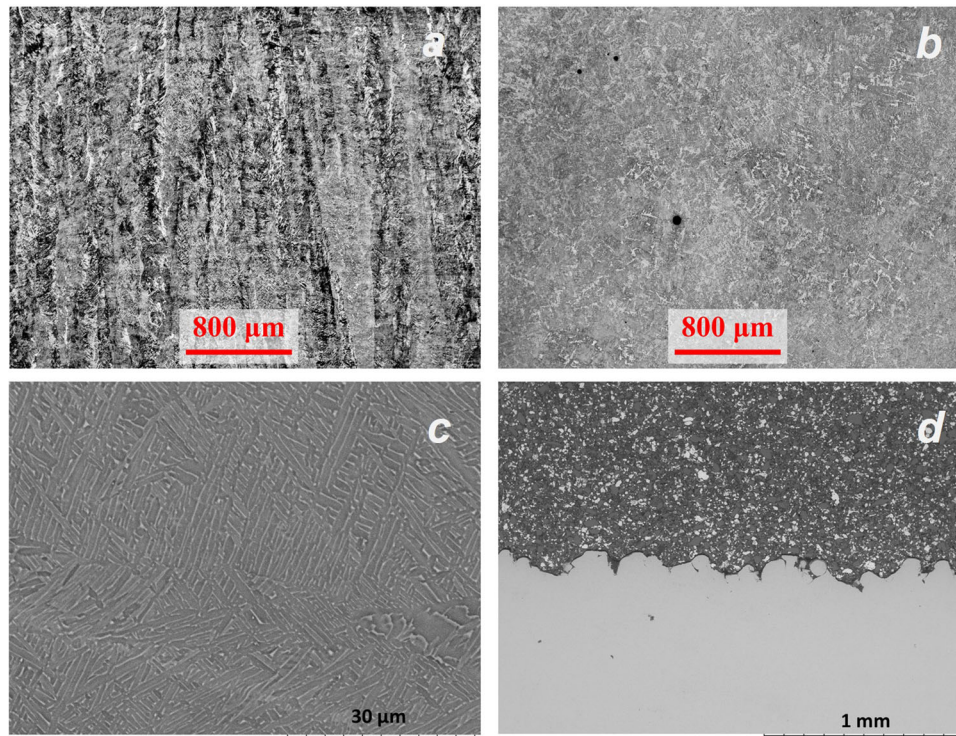


**Fig. 3** (a) Parallel section (b) orthogonal section (c) detailed lamellar microstructure (d) surface profile

after failure. Detailed geometry of the as-built fatigue specimen is reported in Fig. 2.

### 3. Results and Discussion

The microstructure of EBM specimens is made of tiny lamellae of  $\alpha$  phase separated by intergranular  $\beta$  phase (Fig. 3c), indicating fast cooling from temperature above the  $\beta$ -transus. On higher scale the parallel section (Fig. 3a) is made of columnar structure aligned in the direction of heat flow. Those structures represent the  $\beta$  grains that firstly solidify from liquid, then during  $\beta$ -transus the  $\alpha + \beta$  lamellar structure nucleates and grows. The orthogonal section reported in Fig. 3(b) appears homogeneous, some defects like pores are recognizable. The profile of as-built specimen (Fig. 3d) is characterized by the presence of many irregularities like diffused small cracks.

The measured hardness resulted equal to  $331 \pm 3$  HV on the parallel section and  $333 \pm 4$  HV on the orthogonal, these values indicate negligible anisotropy.

The three different treatments are effective in reducing surface roughness as demonstrated by Fig. 3, in the best case analyzed the value of Ra decrease from the initial value of  $7.69 \pm 0.59 \mu\text{m}$  to the final value of  $0.82 \pm 0.03 \mu\text{m}$ .

The reduction in roughness by chemical machining occurs mainly because reaction products accumulate within the valleys where the reaction rate is lower if compared to peaks (Ref (44)).

The roughness reduction occurred mainly in the first 15 min, as reported in Fig. 4, then the roughness decreases slowly toward an asymptotic value, in fact at the beginning the treatment the surface is characterized by deep and sharp valleys and the effect of accumulation of reaction products is maximized, then, as the surface becomes smoother the treatment efficiency decreases.

The final chemically machined surface is characterized by a predominant waviness and the final value of Sa depend mainly on Wa, to this scope the chemical solution is not effective in reducing Wa because waviness surface is made of round and smooth profiles and, as said before, the chemical solution is effective forward sharp profiles.

The presence of waviness also in the case of stagnant condition excludes that it is due to some fluid dynamic cause; however, the origin of waviness is unclear and, probably, it is related to the pre-existing layer by layer structure of the EBM samples. At the end of the chemical treatment the measured roughness of HRS results lower even if comparable to LRS, in both these conditions the final Ra is smaller than stagnant case, instead in terms of Wa no differences are noticed between the three treatments. On the contrary the treatments differ in term of diameter reduction, as showed in Fig. 5(c), the HRS condition results in highest etching rate followed by LRS and ST

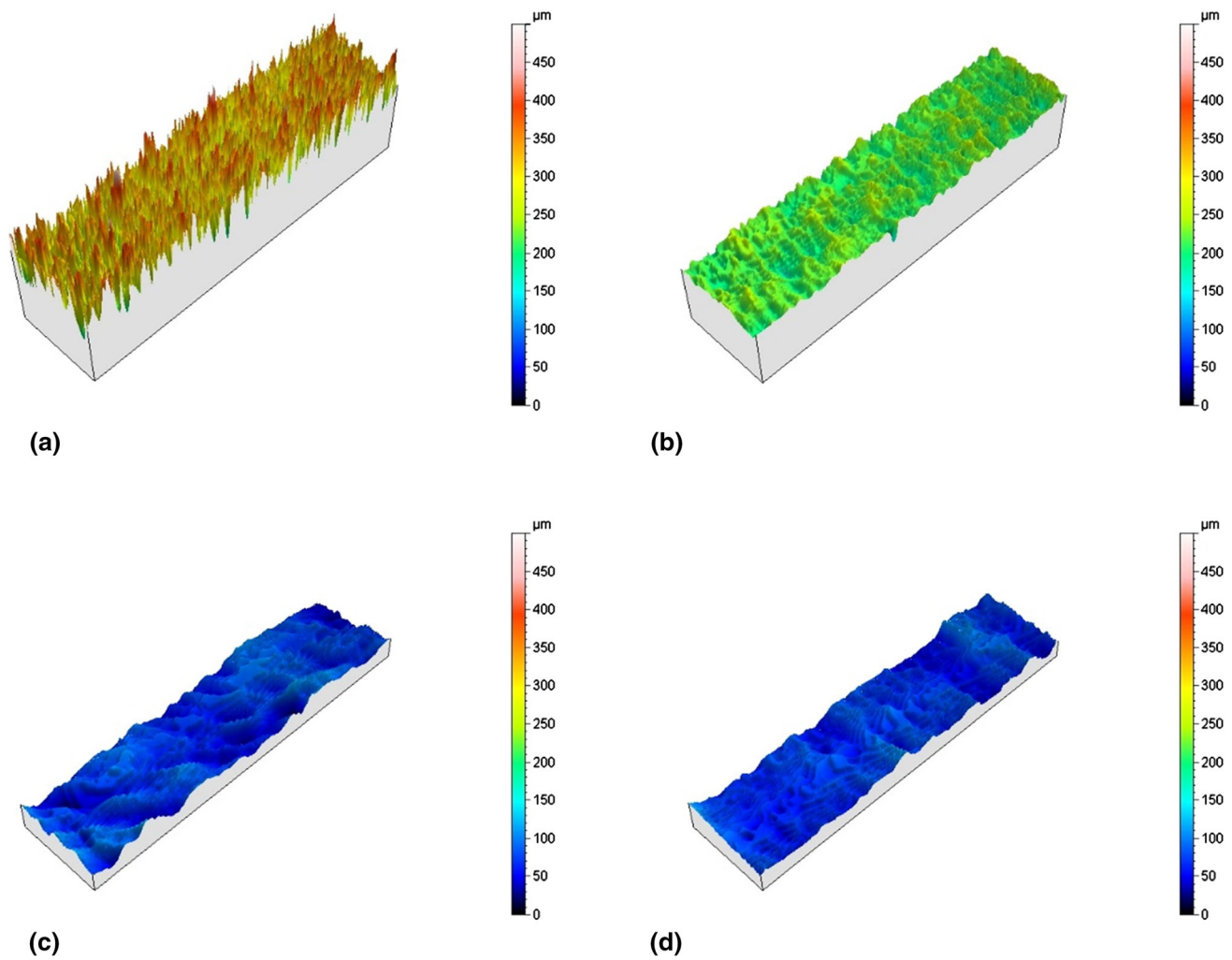


**Fig. 4** (a) Surface morphology and Sa in as-built condition, (b) after ST treatment, (c) after LRS treatment and (d) HRS

The three employed conditions correspond to different fluid dynamics regimes, the evaluated Reynolds numbers for as-built specimen:

$$Re = \frac{\Omega r^2}{\eta}$$

where  $\Omega$  (rad/s) is the angular velocity,  $r$  (m) is the cylinder radius, and  $\eta$  ( $m^2/s$ ) is the kinematic viscosity equal to  $1.4 \times 10^{-6} m^2/s$  in the present case, are reported in Table 2.

Obviously  $Re = 0$  in stagnant condition while LRS correspond to moderate turbulence and HRS to strong turbulence.

In the case of stagnant flow, the mass transfer between the metal surface and solution occurs via molecular diffusion and the concentration gradient on the surface is driving force of the process, in turbulent regimes the diffusion sublayer, i.e., the zone across which mass transfer occurs, depends on  $Re$  and decreases as  $Re$  increases. In smooth surfaces the entire mass transfer between solid and solution is driven by molecular diffusion inside the diffusion sublayer.

Furthermore, if the surface is smooth the diffusion sublayer is well developed and the only effect of increasing  $Re$  is to lower the sublayer thickness, in this way the concentration drop between surface and bulks solution occurs in a smaller distance

with the consequence that the concentration gradient increases and so mass transfer (see Fig. 6a).

Different is the case of rough surfaces, if the roughness is much smaller than the diffusion sublayer thickness, the diffusion sublayer is not perturbed by fluid motion and the mass transfer occurs in the same way of smooth surfaces. However, if roughness is comparable to diffusion sublayer the effect of fluid motion is to break the sublayer; small eddies are generated on the surface and the mass transport mechanism is no more molecular diffusion but convection inside the eddies zone with the effect of increasing mass transfer rate (see Fig. 6b).

In a rough surface made of alternating peaks and valley, the effect of enhanced mass transfer does not concern the fluid inside the valleys where the eddies difficulty penetrates and the fluid is stagnant, but the action of the eddies is strong around the peaks where the dissolution rate is very high.

In the present case the thickness of diffusion sublayer was estimated to be comparable to Sa in both LRS and HRS conditions (Ref (45, 46) The turbulence is responsible to respect stagnant condition to the higher values of etching rate and the lower value of final roughness. Moreover, the increase in turbulence level increases the kinetic energy of eddies and

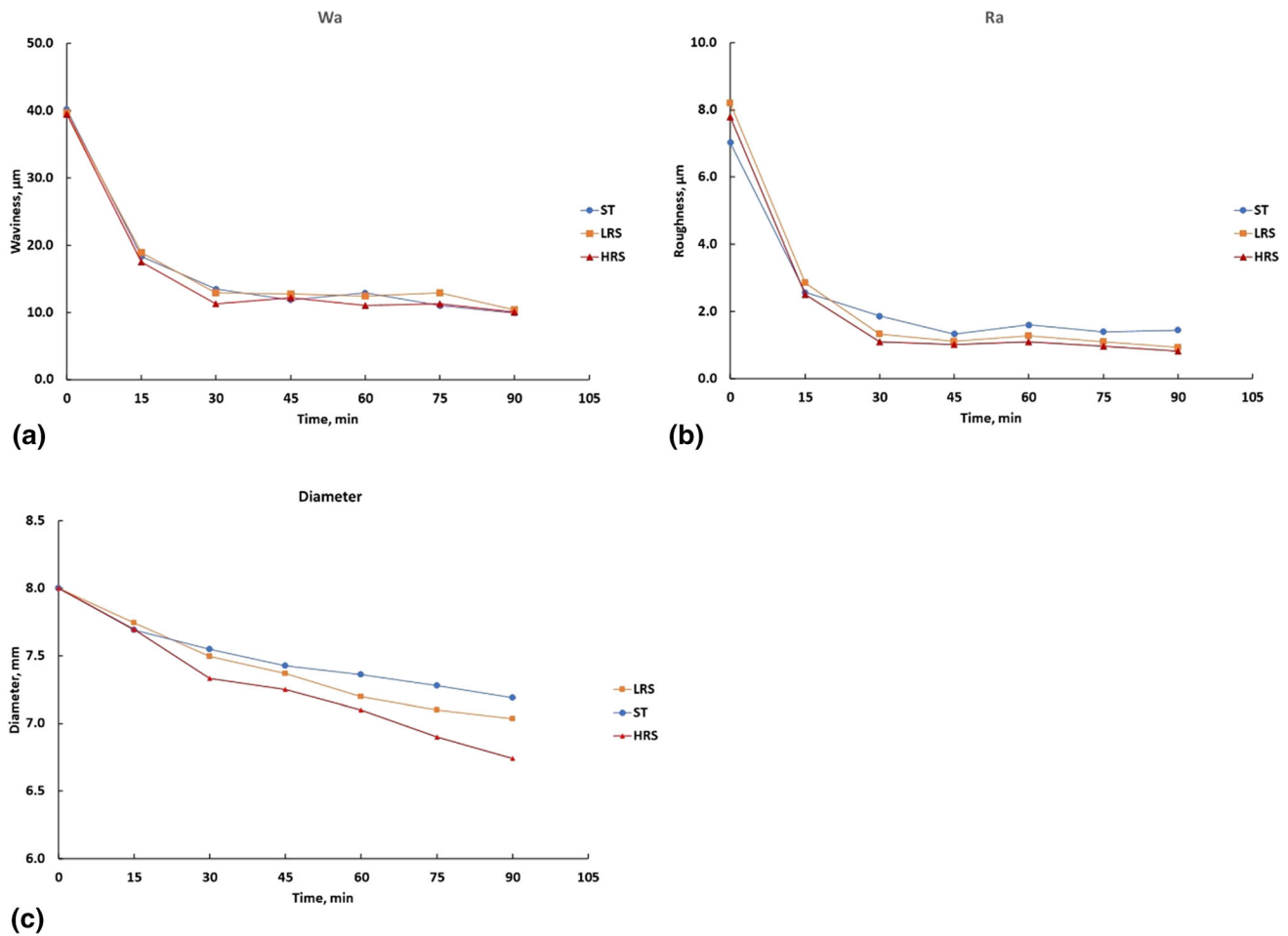


Fig. 5 Trend of (a) Wa, (b) Ra and (c) diameter in ST, LRS and HRS conditions

Table 2 Evaluated Reynolds numbers for the three different conditions

	ST	LRS	HRS
Reynolds number	0	$1.1 \cdot 10^4$	$1.0 \cdot 10^5$

their mass transport capability, the higher turbulence level of HRS condition causes, to respect LRS, the greater etching rate.

Rotating beam fatigue testing has been carried out on both as-built specimens and chemically machined specimens in HRS condition since this condition resulted in the lowest value of Ra and. The chemical treatment results in an enhancement of fatigue behavior, particularly on HCF life, in fact, at the stress level of 300 MPa all the as-built specimens undergo to failure while two treated samples experienced runout and the third failed at about  $2 \times 10^6$  cycles as shown in Fig. 7.

Fracture surfaces was analyzed to highlight their main features and treatment influence. Depending on the stress level and starting surface quality, it is possible to highlight the differences between treated and untreated fracture surfaces after fatigue testing.

Specimens subjected to the maximum stress (900 MPa) exhibit different fracture surfaces, particularly the as-built case has multiple crack initiation sites evidenced by a circular shiny zone on the outer part of the surface, the multiple crack

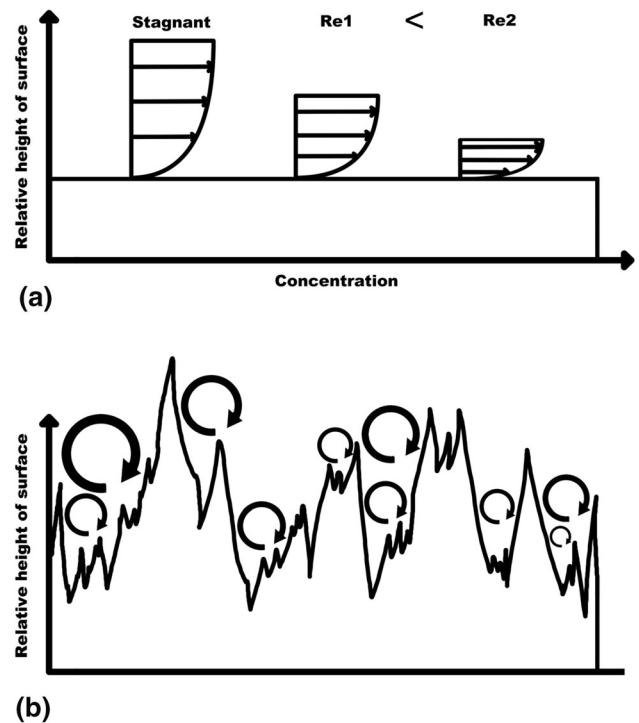
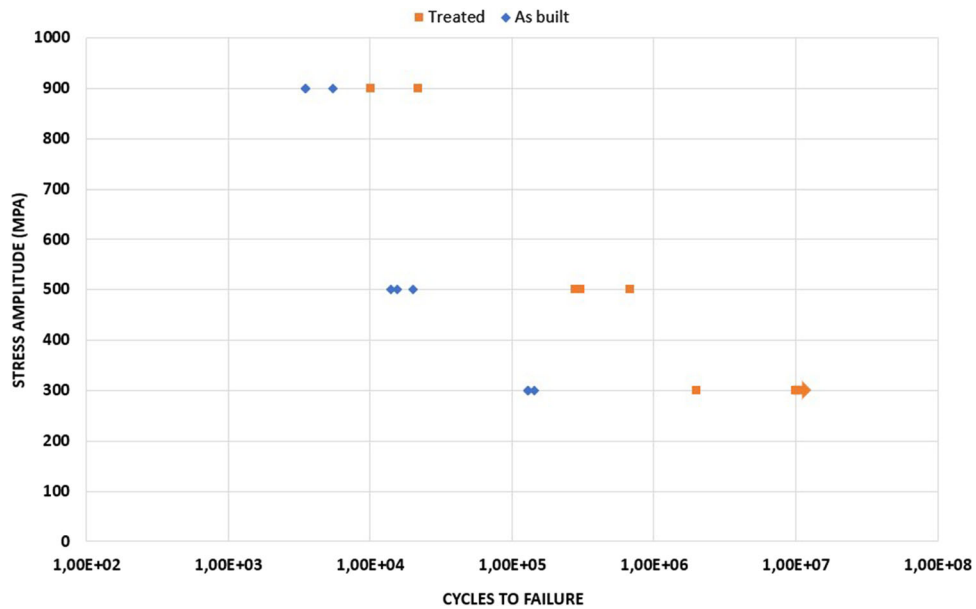


Fig. 6 (a) effect of Reynolds number on diffusion sublayer thickness on smooth surfaces; (b) formation of turbulent eddies on rough surface



**Fig. 7** Whoeler's curves for treated and as-built Ti6Al4V EBM fatigue specimens

initiation observed is compatible with the profile reported in Fig. 3(b); the treated part, instead has different shiny areas originated by single defects, superficial or sub-superficial, brought to surface by the chemical treatment. In this case, the fracture surface is more like a mild stress concentration case.

The stress of 500 MPa results in a similar surface morphology to the case of 900 MPa with a small difference on the dimensions of crack propagation and failure areas. Also in this case, the untreated specimen is characterized by a shiny circular zone while the treated specimen has evident tracks of crack propagation originated from metallurgical defects.

Finally, the 300 MPa stress level was enough for detecting failure in untreated specimens while a fatigue limit is found for treated specimens. However, one of the three treated parts failed prematurely because of a big pore brought to surface from the treatment, the pore is evident in both Fig. 8(d) and 9(b).

A SEM inspection is capable of further detailing the different cracking initiation system, as shown in Fig. 9. Image (a) shows the multi cracking system typical of the untreated specimens while image (b) highlights the cracking initiation from single defects. Image (c) and (d), respectively, represent the crack propagation and fracture zone which are similar on both treated and untreated specimens. The propagation area is characterized by the typical morphology deriving from  $R = -1$  fatigue stress type, exhibiting compression bands deriving from the alternate stress. The fracture zone, instead, is characterized by dimples typical of a ductile failure.

To sum up, for untreated specimens, cracking initiates from multiple superficial sites, while for treated parts cracking always initiates from a specific site (generally a superficial/sub-superficial flaw).

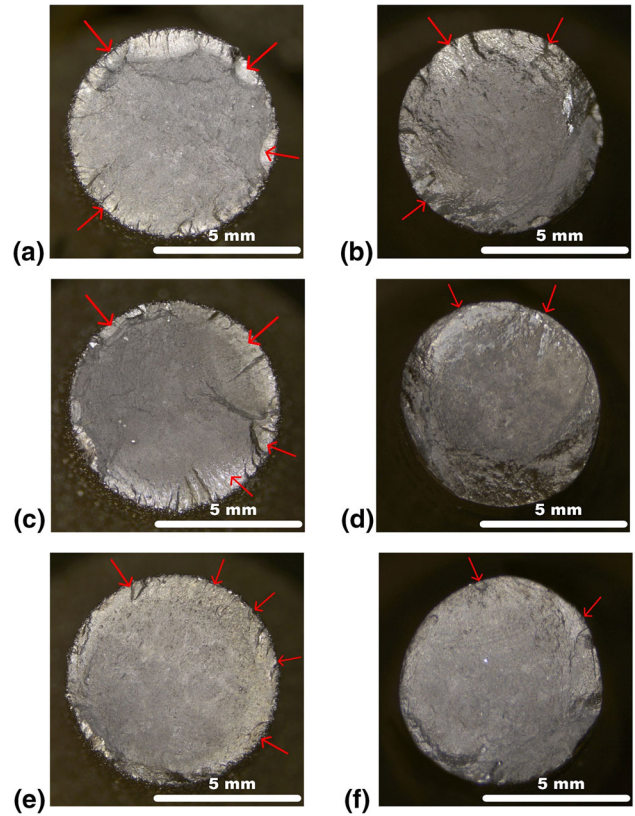


**Fig. 8** Comparison between as-built and treated specimen fracture surface, at different stress levels: (a) as-built specimen stressed at 900 MPa; (b) treated specimen stressed at 900 MPa; (c) as-built specimen stressed at 500 MPa; (d) treated specimen stressed at 500 MPa; (e) as-built specimen stressed at 300 MPa; (f) premature failure of treated specimen stressed at 300 MPa

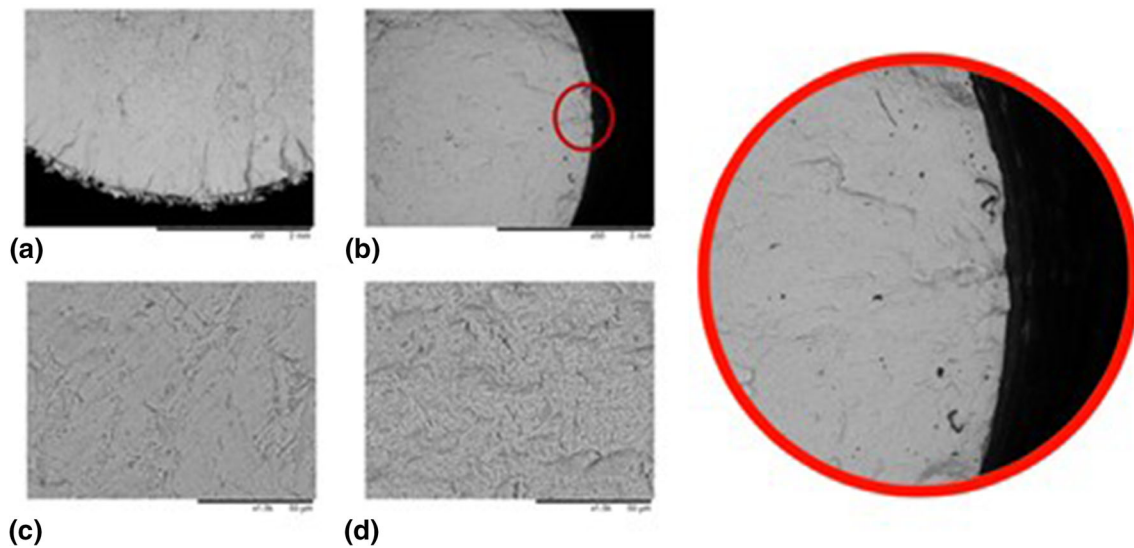


**Fig. 9** SEM acquisitions: (a) crack initiation on surface for untreated specimen; (b) crack initiation site from metallurgical defect near surface for treated specimen; (c) crack propagation zone; (d) fracture zone

## 4. Conclusions

Considering the findings of this study, the following conclusions can be made:

1. Chemical machining is capable to improve the surface quality of Ti6Al4V specimen produced by EBM. In all the three analyzed conditions the roughness is considerably reduced; however, at the end of the treatment the surface is characterized by predominant waviness. The waviness is not related to some fluid dynamic effects since it develops also in stagnant conditions, it is, probably, related to the pre-existing layer by layer structure of the EBM samples. At high Reynolds number the turbulence generates eddies that break the diffusion sublayer and increase the mass transfer rate. The eddies, also, enhance the selectivity forward peaks of the process.
2. Compared to untreated specimens, the fatigue behavior of treated specimens shows improved results particularly in HCF. The negative effects of poor surface quality on fatigue life are mitigated by chemical treatment; however, crack initiation is always associated with a surface/sub-surface defect. The occurrence and size of defects can be reduced by improving the quality of the base material prior to treatment.

## Funding

Open access funding provided by Università degli Studi di Napoli Federico II within the CRUI-CARE Agreement.

## Open Access

This article is licensed under a Creative Commons Attribution 4.0 International License, which permits use, sharing, adaptation,

distribution and reproduction in any medium or format, as long as you give appropriate credit to the original author(s) and the source, provide a link to the Creative Commons licence, and indicate if changes were made. The images or other third party material in this article are included in the article's Creative Commons licence, unless indicated otherwise in a credit line to the material. If material is not included in the article's Creative Commons licence and your intended use is not permitted by statutory regulation or exceeds the permitted use, you will need to obtain permission directly from the copyright holder. To view a copy of this licence, visit <http://creativecommons.org/licenses/by/4.0/>.

## References

1. W.E. Frazier, Metal Additive Manufacturing: A Review, *J. Mater. Eng. Perform.*, 2014, **23**(6), p 1917–1928.
2. H. Fayazfar, J. Sharifi, M.K. Keshavarz, and M. Ansari, “An Overview of Surface Roughness Enhancement of Additively Manufactured Metal Parts: A Path towards Removing the Post-Print Bottleneck for Complex Geometries, *Int. J. Adv. Manuf. Technol.*, 2023 <https://doi.org/10.1007/s00170-023-10814-6>
3. J. Boban, A. Ahmed, E.K. Jithinraj, M.A. Rahman, and M. Rahman, “Polishing of Additive Manufactured Metallic Components: Retrospect on Existing Methods and Future Prospects, *Int. J. Adv. Manuf. Technol.*, 2022 <https://doi.org/10.1007/s00170-022-09382-y>
4. C. Wei, Z. Zhang, D. Cheng, Z. Sun, M. Zhu, and L. Li, An Overview of Laser-Based Multiple Metallic Material Additive Manufacturing: From Macro- to Micro-Scales, *Int. J. Extrem. Manuf.*, 2020, **3**(1), p 12003.
5. X. Gong, T. Anderson, and K. Chou, *Review on Powder-Based Electron Beam Additive Manufacturing Technology*, 2012 <https://doi.org/10.1115/ISFA2012-7256>
6. A.H. Chern, P. Nandwana, T. Yuan, M.M. Kirka, R.R. Dehoff, P.K. Liaw, and C.E. Duty, A Review on the Fatigue Behavior of Ti-6Al-4V Fabricated by Electron Beam Melting Additive Manufacturing, *Int. J. Fatigue*, 2019, **119**, p 173–184. <https://doi.org/10.1016/j.ijfatigue.2018.09.022>
7. E. Manco, E. Cozzolino, and A. Astarita, Laser Polishing of Additively Manufactured Metal Parts: A Review, *Surf. Eng.*, 2022 <https://doi.org/10.1080/02670844.2022.2072080>
8. S. Liu and Y.C. Shin, Additive Manufacturing of Ti6Al4V Alloy: A Review, *Mater. Des.*, 2019, **164**, p 107552. <https://doi.org/10.1016/j.matdes.2018.107552>
9. A. Fatemi, R. Molaei, J. Simsirivong, N. Sanaei, J. Pegues, B. Torries, N. Phan, and N. Shamsaei, Fatigue Behaviour of Additive Manufac-



- tured Materials: An Overview of Some Recent Experimental Studies on Ti-6Al-4V Considering Various Processing and Loading Direction Effects, *Fatigue Fract. Eng. Mater. Struct. Fract. Eng. Mater. Struct.*, 2019, **42**(5), p 991–1009.
10. J. Gockel, L. Sheridan, B. Koerper, and B. Whip, The Influence of Additive Manufacturing Processing Parameters on Surface Roughness and Fatigue Life, *Int. J. Fatigue*, 2019, **124**, p 380–388. <https://doi.org/10.1016/j.ijfatigue.2019.03.025>
  11. A. Yadollahi and N. Shamsaei, Additive Manufacturing of Fatigue Resistant Materials: Challenges and Opportunities, *Int. J. Fatigue*, 2017, **98**, p 14–31. <https://doi.org/10.1016/j.ijfatigue.2017.01.001>
  12. A. Cutolo, C. Elangeswaran, G.K. Muralidharan, and B. Van Hooreweder, On the Role of Building Orientation and Surface Post-Processes on the Fatigue Life of Ti-6Al-4V Coupons Manufactured by Laser Powder Bed Fusion, *Mater. Sci. Eng. A*, 2022, **840**, 142747. <https://doi.org/10.1016/j.msea.2022.142747>
  13. D. Crococolo, M. De Agostinis, S. Fini, G. Olmi, A. Vranic, and S. Ciric-Kostic, Influence of the Build Orientation on the Fatigue Strength of EOS Maraging Steel Produced by Additive Metal Machine, *Fatigue Fract. Eng. Mater. Struct. Fract. Eng. Mater. Struct.*, 2016, **39**(5), p 637–647.
  14. P.D. Nezhadfar, R. Shrestha, N. Phan, and N. Shamsaei, Fatigue Behavior of Additively Manufactured 17–4 PH Stainless Steel: Synergistic Effects of Surface Roughness and Heat Treatment, *Int. J. Fatigue*, 2019, **124**, p 188–204. <https://doi.org/10.1016/j.ijfatigue.2019.02.039>
  15. A. Tridello, J. Fiocchi, C.A. Biffi, G. Chiandussi, M. Rossetto, A. Tuissi, and D.S. Paolino, VHCF Response of Gaussian SLM AlSi10Mg Specimens: Effect of a Stress Relief Heat Treatment, *Int. J. Fatigue*, 2019, **124**, p 435–443. <https://doi.org/10.1016/j.ijfatigue.2019.02.020>
  16. T.M. Mower and M.J. Long, Mechanical Behavior of Additive Manufactured, Powder-Bed Laser-Fused Materials, *Mater. Sci. Eng. A*, Elsevier, 2016, **651**, p 198–213, doi:<https://doi.org/10.1016/j.msea.2015.10.068>
  17. P.A. Kobryn and S.L. Semiatin, Mechanical Properties of Laser-Deposited Ti-6Al-4V P.A. Kobryn and S.L. Semiatin Air Force Research Laboratory, AFRL/MLLMP, Wright-Patterson Air Force Base, OH 45433-7817, *Int. Solid Free. Fabr. Symp.*, 2001, p 179–186
  18. W. Du, Q. Bai, and B. Zhang, A Novel Method for Additive/Subtractive Hybrid Manufacturing of Metallic Parts, *Procedia Manuf.*, 2016, **5**, p 1018–1030. <https://doi.org/10.1016/j.promfg.2016.08.067>
  19. A.H. Maamoun, M.A. Elbestawi, and S.C. Veldhuis, Influence of Shot Peening on AlSi10Mg Parts Fabricated by Additive Manufacturing, *J. Manuf. Mater. Process.*, 2018 <https://doi.org/10.3390/jmmp2030040>
  20. B. AlMangour and J.-M. Yang, Improving the Surface Quality and Mechanical Properties by Shot-Peening of 17–4 Stainless Steel Fabricated by Additive Manufacturing, *Mater. Des.*, 2016, **110**, p 914–924. <https://doi.org/10.1016/j.matdes.2016.08.037>
  21. M.A. Bernevig-Sava, C. Stamate, N.M. Lohan, A.M. Baci, I. Postolache, C. Baci, and E.R. Baci, Considerations on the Surface Roughness of SLM Processed Metal Parts and the Effects of Subsequent Sandblasting, *IOP Conf. Ser. Mater. Sci. Eng.*, 2019, **572**(1)
  22. M. Barletta, Progress in Abrasive Fluidized Bed Machining, *J. Mater. Process. Technol.*, 2009, **209**(20), p 6087–6102.
  23. E. Atzeni, M. Barletta, F. Calignano, L. Iuliano, G. Rubino, and V. Tagliaferri, Abrasive Fluidized Bed (AFB) Finishing of AlSi10Mg Substrates Manufactured by Direct Metal Laser Sintering (DMLS), *Addit. Manuf. Manuf.*, 2016, **10**, p 15–23. <https://doi.org/10.1016/j.addma.2016.01.005>
  24. A.P. Nagalingam, H.K. Yuvaraj, and S.H. Yeo, Synergistic Effects in Hydrodynamic Cavitation Abrasive Finishing for Internal Surface-Finish Enhancement of Additive-Manufactured Components, *Addit. Manuf. Manuf.*, 2020, **33**, 101110. <https://doi.org/10.1016/j.addma.2020.101110>
  25. J. Guo, C. Song, Y. Fu, K.H. Au, C.W. Kum, M.H. Goh, T. Ren, R. Huang, and C.-N. Sun, Internal Surface Quality Enhancement of Selective Laser Melted Inconel 718 by Abrasive Flow Machining, *J. Manuf. Sci. Eng.*, 2020, **142**(10)
  26. X. Zhang and L. Chen, Effects of Laser Scanning Speed on Surface Roughness and Mechanical Properties of Aluminum/Poly(lactic Acid (Al/PLA) Composites Parts Fabricated by Fused Deposition Modeling, *Polym. Test. Test.*, 2020, **91**, p 106785. <https://doi.org/10.1016/j.polymeresting.2020.106785>
  27. K.C. Yung, T.Y. Xiao, H.S. Choy, W.J. Wang, and Z.X. Cai, Laser Polishing of Additive Manufactured CoCr Alloy Components with Complex Surface Geometry, *J. Mater. Process. Technol.*, 2018, **262**(Jan), p 53–64. <https://doi.org/10.1016/j.jmatprotec.2018.06.019>
  28. X. Chen, B. Chen, X. Cheng, G. Li, and Z. Huang, Microstructure and Properties of Hybrid Additive Manufacturing 316L Component by Directed Energy Deposition and Laser Remelting, *J. Iron. Steel Res. Int.*, 2020, **27**(7), p 842–848. <https://doi.org/10.1007/s42243-020-00396-y>
  29. J. Guo, M.H. Goh, P. Wang, R. Huang, X. Lee, B. Wang, S.M.L. Nai, and J. Wei, Investigation on Surface Integrity of Electron Beam Melted Ti-6Al-4 V by Precision Grinding and Electropolishing, *Chinese J. Aeronaut.*, 2021, **34**(12), p 28–38.
  30. F. Scherillo, Chemical Surface Finishing of AlSi10Mg Components Made by Additive Manufacturing, *Manuf. Lett.*, 2019, **19**, p 5–9. <https://doi.org/10.1016/j.mfglet.2018.12.002>
  31. F. Scherillo, E. Manco, A. El Hassanin, S. Franchitti, C. Pirozzi, and R. Borrelli, Chemical Surface Finishing of Electron Beam Melted Ti6Al4V Using HF-HNO<sub>3</sub> Solutions, *J. Manuf. Process.*, 2020, **60**(Oct), p 400–409. <https://doi.org/10.1016/j.jmapro.2020.10.033>
  32. B. Wysocki, J. Idaszek, J. Buhagiar, K. Szlązak, T. Brynk, K.J. Kurzydłowski, and W. Świąszkowski, The Influence of Chemical Polishing of Titanium Scaffolds on Their Mechanical Strength and In-Vitro Cell Response, *Mater. Sci. Eng. C*, 2019, **95**, p 428–439.
  33. M.A. Obeidi, A. Mussatto, M.N. Dogu, S.P. Sreenilayam, E. McCarthy, I.U. Ahad, S. Keaveney, and D. Brabazon, Laser Surface Polishing of Ti-6Al-4V Parts Manufactured by Laser Powder Bed Fusion, *Surf. Coatings Technol.*, 2022, **434**, 128179
  34. P. Edwards and M. Ramulu, Fatigue Performance Evaluation of Selective Laser Melted Ti-6Al-4V, *Mater. Sci. Eng. A*, 2014, **598**, p 327–337. <https://doi.org/10.1016/j.msea.2014.01.041>
  35. P.E. Carrion, N. Shamsaei, S.R. Daniewicz, and R.D. Moser, Fatigue Behavior of Ti-6Al-4V ELI Including Mean Stress Effects, *Int. J. Fatigue*, 2016, **2017**(99), p 87–100.
  36. M. Bezuidenhout, G. Ter Haar, T. Becker, S. Rudolph, O. Damm, and N. Sacks, The Effect of HF-HNO<sub>3</sub> Chemical Polishing on the Surface Roughness and Fatigue Life of Laser Powder Bed Fusion Produced Ti6Al4V, *Mater. Today Commun.*, 2020, **25**(1), p 101396. <https://doi.org/10.1016/j.mtcomm.2020.101396>
  37. Ł. Zrodowski, T. Choma, I. Wilkos, and A. Kurek, Influence of Surface Characteristics and Finishing on Fatigue Properties of Additively Manufactured Ti6Al4V, in *2021 6th International Conference on Nanotechnology for Instrumentation and Measurement (NanofIM)*, 2021, p 1–4
  38. L. Rony, E. Aguado, B. Verlee, F. Pascaretti-Grizon, and D. Chappard, Osseointegration of Two Types of Titanium Cylinders with Geometric or Trabecular Microarchitecture: A Nanotomographic and Histomorphometric Study, *Morphologie*, 2022, **106**(353), p 80–91. <https://doi.org/10.1016/j.morpho.2021.03.001>
  39. L. Di Angelo, P. Di Stefano, and E. Guardiani, Search for the Optimal Build Direction in Additive Manufacturing Technologies: A Review, *J. Manuf. Mater. Process.*, 2020, **4**(3)
  40. S. Franchitti, C. Pirozzi, and R. Borrelli, Influence of Hot Isostatic Pressing and Surface Finish on the Mechanical Behaviour of Ti6Al4V Processed by Electron Beam Melting, *Fatigue Fract. Eng. Mater. Struct. Fract. Eng. Mater. Struct.*, 2020, **43**(12), p 2828–2841.
  41. E. Manco, F. Scherillo, C. Guerrero, M. Bruno, A. El Hassanin, S. Franchitti, R. Borrelli, and L. Esposito, Influence of Chemical Machining on Axial Fatigue Behaviour of Electron Beam Melted Ti6Al4V Parts, *Manuf. Lett.*, 2023, **35**, p 6–10. <https://doi.org/10.1016/j.mfglet.2022.11.001>
  42. M. Kahlin, H. Ansell, and J.J. Moverare, Fatigue Behaviour of Notched Additive Manufactured Ti6Al4V with As-Built Surfaces, *Int. J. Fatigue*, 2017, **101**, p 51–60. <https://doi.org/10.1016/j.ijfatigue.2017.04.009>
  43. D. Greitemeier, C.D. Donne, F. Syassen, J. Eufinger, and T. Melz, Effect of Surface Roughness on Fatigue Performance of Additive Manufactured Ti-6Al-4V, *Mater. Sci. Technol.*, 2016, **32**(7), p 629–634. <https://doi.org/10.1179/1743284715Y.0000000053>
  44. B. Chatterjee, Chemical Brightening of Aluminium, *Mater. Chem. Phys.*, 1984

45. B. Evgeny, T. Hughes, and D. Eskin, Effect of Surface Roughness on Corrosion Behaviour of Low Carbon Steel in Inhibited 4 M Hydrochloric Acid under Laminar and Turbulent Flow Conditions, *Corros. Sci.*, 2016, **103**, p 196–205.
46. Transport Phenomena, R. B. Bird, W. E. Stewart, and E. N. Lightfoot, Wiley, New York (1960). 780 Pages. \$11.50, *AIChE J.*, 1961, **7**(2), p 5J-6J

**Publisher's Note** Springer Nature remains neutral with regard to jurisdictional claims in published maps and institutional affiliations.